Analytical and Numerical Solutions for Nonlinear Equations
©Available online at https://ansne.du.ac.ir/
Online ISSN: 3060–785X
2025, Volume 10, Issue 1, pp. 91–99
Research article

A Non-Linear Equation for Entanglement Entropy: Analytical and Numerical Approaches

Fabiano F. Santos*

[1] Centro de Ciências Exatas, Naturais e Tecnológicas, UEMASUL, 65901-480, Imperatriz, MA, Brazil

[2] Departamento de Física, Universidade Federal do Maranhão, São Luís, 65080-805, Brazil

* **Corresponding author(s):** fabiano.ffs23@gmail.com

Received: 18/09/2025 **Accepted:** 15/12/2025 **Published:** 17/12/2025 10.22128/ansne.2025.3059.1157

Abstract

We study a non-linear equation arising in the computation of entanglement entropy in interacting quantum systems. Motivated by field-theoretic and holographic models, we propose a simplified non-linear differential equation for the entropy as a function of subsystem size and coupling strength. Analytical approximations are compared with numerical solutions, and the resulting behavior suggests a crossover between area-law and volume-law regimes. This work provides a minimal model for capturing the non-linear structure of entanglement dynamics.

Keywords: Entanglement entropy, Quantum information, Non-linear equations.

Mathematics Subject Classification (2020): 81P45, 35A25, 35Q40

1 Introduction

Entanglement entropy has become one of the most widely used quantitative measures of quantum correlations in both condensed matter physics and high-energy theory. Originally introduced in the study of black hole thermodynamics [1, 2], where it offered a statistical explanation for the Bekenstein–Hawking entropy, the concept was later adapted to characterize the scaling of quantum correlations in extended many-body systems [3,4]. For a bipartition of a system into region A and its complement B, the entanglement entropy is defined as the von Neumann entropy $S_A = -\mathrm{Tr}(\rho_A \ln \rho_A)$ of the reduced density matrix ρ_A, and it reflects how strongly the two regions are entangled.

In one spatial dimension, conformal field theory (CFT) methods have allowed for exact calculations of entanglement entropy, showing that S_A grows logarithmically with subsystem size at criticality [5, 6]. In higher dimensions, the generic scaling law is that of an "area law," where the entropy grows with the size of the boundary of A rather than its volume [3]. Yet, important exceptions to the area law exist. Systems with Fermi surfaces [7, 8], disordered or many-body localized phases [9], and holographic theories with strongly coupled duals [10,11] all exhibit corrections or departures from this naive scaling. As a result, understanding how entanglement entropy interpolates between different scaling regimes remains a problem of continuing interest.

One of the most persistent challenges is that exact expressions for entanglement entropy are rarely available outside of special cases, forcing researchers to rely on effective equations, variational principles, or numerical approaches. For instance, in the holographic

setting, the celebrated Ryu–Takayanagi formula reduces the computation of entanglement entropy to solving extremal surface equations in higher-dimensional curved spacetimes, which are inherently non-linear [10,11]. In condensed matter physics, tensor network approaches [12,13] and replica field theory methods [14] also introduce non-linear structures when attempting to resum higher-order contributions or approximate entanglement growth in interacting systems.

The present work takes a complementary point of view. Rather than attempting to derive the entropy from first principles in a microscopic theory, we propose to study a phenomenological non-linear equation that governs the entropy $S(\ell)$ as a function of subsystem size ℓ. The idea is to capture qualitative features such as the crossover from logarithmic scaling to saturation by solving and analyzing a single effective equation. This approach mirrors similar efforts in statistical physics and mathematical biology, where non-linear ordinary differential equations provide tractable minimal models of complex emergent phenomena. By analyzing the solutions of such an equation, we aim to identify the simplest mathematical structures capable of interpolating between the different asymptotic regimes of entanglement entropy.

The paper is organized as follows. In Sec. 2 we introduce the nonlinear differential equation for the entanglement entropy and explain its physical motivation. In Sec. 3 we develop exact integral relations and controlled analytical approximations, highlighting the resulting universality classes. Sec. 4 presents a detailed numerical study that corroborates the analytical predictions and quantifies the accuracy of closed-form approximants. In Sec. 5 we have discussion and conclusions, emphasizing the broader implications of the model and outlining future directions.

2 The Non-Linear Equation

Our starting point is the hypothesis that the entanglement entropy $S(\ell)$ of an interval of length ℓ in a one-dimensional system, or more generally of a subsystem of characteristic size ℓ, obeys an effective evolution equation of non-linear type. The form of the equation is guided by three minimal physical requirements:

(i) For small ℓ, the entropy should grow monotonically and, in critical systems, approach logarithmic behavior consistent with conformal field theory.

(ii) At large ℓ, saturation or sublinear growth should occur, reflecting finite correlation length or finite total entropy capacity.

(iii) The dynamics of $S(\ell)$ should be governed by a local equation in ℓ, depending only on S and its derivatives at that point.

The simplest equation consistent with these requirements is a second-order non-linear ordinary differential equation of Riccati-type,

$$\frac{d^2S}{d\ell^2}+\alpha\left(\frac{dS}{d\ell}\right)^2-\beta e^{-S(\ell)}=0, \tag{1}$$

where $\alpha,\beta>0$ are phenomenological constants. The term quadratic in $S'(\ell)$ is motivated by the analogy with semiclassical gravity equations, where backreaction effects lead to quadratic non-linearities [10]. The exponential term $-\beta e^{-S(\ell)}$ ensures saturation at large S, mimicking the suppression of entropy growth once correlations have spread across the entire system.

To analyze Eq. (1), it is convenient to define the entropy rate

$$u(\ell)=\frac{dS}{d\ell}. \tag{2}$$

Equation (1) becomes

$$\frac{du}{d\ell}+\alpha u^2-\beta e^{-S}=0. \tag{3}$$

Since $dS/d\ell=u$, we can use the chain rule $\frac{du}{d\ell}=\frac{du}{dS}\frac{dS}{d\ell}=u\frac{du}{dS}$, leading to an autonomous first-order equation:

$$u\frac{du}{dS}+\alpha u^2-\beta e^{-S}=0. \tag{4}$$

This is a nonlinear Bernoulli-type equation for $u(S)$. Rearranging,

$$\frac{du}{dS}=-\alpha u+\frac{\beta}{u}e^{-S}. \tag{5}$$

Equation (4) can be interpreted as a dynamical system in the (S,u) plane, where the entropy growth rate interacts with the entropy itself through exponential feedback.

Multiplying Eq. (4) by u and rearranging, we obtain

$$\frac{1}{2}\frac{d}{dS}(u^2)+\alpha u^2=\beta e^{-S}. \tag{6}$$

This is a first-order linear inhomogeneous equation for $u^2(S)$, which admits an exact solution. Introducing $v(S)=u^2(S)$, we have

$$\frac{dv}{dS}+2\alpha v=2\beta e^{-S}. \tag{7}$$

The integrating factor is $e^{2\alpha S}$, so

$$\frac{d}{dS}\left(ve^{2\alpha S}\right)=2\beta e^{(2\alpha-1)S}. \tag{8}$$

Integrating yields

$$v(S)e^{2\alpha S}=\frac{2\beta}{2\alpha-1}e^{(2\alpha-1)S}+C, \tag{9}$$

where C is an integration constant determined by initial conditions. Therefore,

$$u^2(S)=\frac{2\beta}{2\alpha-1}e^{-S}+Ce^{-2\alpha S}. \tag{10}$$

Equation (10) is the central result: it provides an exact integral relation between entropy S and its derivative $u=dS/d\ell$. In particular, it shows that the square of the growth rate decomposes into two contributions: one exponential in $-S$ and another suppressed as $e^{-2\alpha S}$.

Equation (10) implies distinct asymptotic regimes:

Small S regime. For $S\ll 1$, the exponential factors are close to unity, and $u^2\approx\frac{2\beta}{2\alpha-1}+C$. Thus the entropy initially grows nearly linearly in ℓ, consistent with short-range expansion.

Intermediate regime. As S increases, the e^{-S} term dominates while the $e^{-2\alpha S}$ contribution is suppressed more rapidly. This gives

$$\frac{dS}{d\ell}\approx\sqrt{\frac{2\beta}{2\alpha-1}}e^{-S/2}, \tag{11}$$

which integrates to

$$S(\ell)\approx 2\ln\left(\sqrt{\frac{\beta}{2\alpha-1}}\,\ell+\text{const}\right). \tag{12}$$

This reproduces logarithmic growth of entropy with ℓ, consistent with conformal field theory predictions.

Large S regime. For very large S, both exponential contributions vanish, and the differential equation implies $u\to 0$. Thus entropy saturates, approaching a finite value. This is consistent with finite system size or finite correlation length.

The derivation of Eq. (10) provides a non-trivial check that the phenomenological model captures known behaviors: linear onset, logarithmic growth, and eventual saturation. Moreover, the presence of the integration constant C indicates sensitivity to microscopic boundary conditions. For $\alpha=1/2$, the derivation would break down due to resonance, suggesting a special scaling case where corrections may take power-law rather than logarithmic form.

This analysis demonstrates that even a simple non-linear model admits rich mathematical structure, directly connecting to scaling laws observed in critical and non-critical quantum systems.

Equation (4) defines a dynamical system in the (S,u) plane:

$$\frac{dS}{d\ell}=u, \tag{13}$$

$$\frac{du}{d\ell}=-\alpha u^2+\beta e^{-S}. \tag{14}$$

This is equivalent to a two-dimensional autonomous system, whose trajectories describe the evolution of entropy and its rate of change. Phase-plane methods allow us to extract qualitative properties of solutions without explicit integration.

The fixed points of the system are given by $u = 0$ and $\beta e^{-S} = 0$. Since $\beta > 0$, the only fixed points occur at $u = 0$ and $S \to \infty$. In other words, the entropy tends toward saturation at large ℓ, where the growth rate u vanishes. No finite-S fixed point exists, reflecting the monotonic growth of entanglement entropy with subsystem size.

To examine the stability, linearize around $u = 0$ with S finite:

$$\frac{du}{d\ell} \approx \beta e^{-S}. \tag{15}$$

This shows that u grows linearly away from zero at small S, confirming that $u = 0$ is not stable at finite S. However, at large S, the driving term βe^{-S} decays exponentially, and u asymptotically approaches zero. Thus $u = 0$ at $S \to \infty$ is an attractive asymptotic state.

From Eq. (10), trajectories in the (S,u) plane lie on curves of the form

$$u^2(S) = \frac{2\beta}{2\alpha - 1} e^{-S} + Ce^{-2\alpha S}, \tag{16}$$

with constant C. These curves define invariant manifolds of the dynamical system, parameterized by C. Each trajectory corresponds to a different microscopic initialization of the entanglement growth, such as boundary conditions or coupling strength.

Depending on the sign of the integration constant C, distinct families of solutions emerge:

- **Positive-C branch:** If $C > 0$, the second term in Eq. (10) contributes positively. This yields faster initial growth of $u(\ell)$ and delayed saturation of $S(\ell)$. Physically, this corresponds to systems with stronger short-range correlations, where entanglement spreads more rapidly.

- **Negative-C branch:** If $C < 0$, then $u^2(S)$ is reduced. This corresponds to slower initial growth and earlier onset of saturation. In the extreme case where C cancels the e^{-S} contribution at small S, the entropy may remain nearly constant, modeling weakly entangled or gapped phases.

- **Critical branch:** For $C = 0$, only the universal e^{-S} term remains. This branch corresponds to a scaling solution interpolating between logarithmic growth and saturation. It can be viewed as the "critical manifold" of the system.

The derivation of Eq. (10) assumed $2\alpha \neq 1$. If $\alpha = \frac{1}{2}$, the integration of the first-order equation leads instead to

$$\frac{dv}{dS} + v = 2\beta e^{-S}, \qquad v = u^2. \tag{17}$$

This integrates to

$$v(S)e^{S} = 2\beta S + C, \tag{18}$$

or equivalently

$$u^2(S) = \frac{2\beta S + C}{e^{S}}. \tag{19}$$

Unlike the generic case, here the prefactor grows linearly in S before being suppressed by the exponential denominator. This leads to slower decay of u at intermediate scales and suggests a distinct scaling law:

$$S(\ell) \sim \ln \ell + \ln\ln \ell, \tag{20}$$

up to constants. Thus $\alpha = \frac{1}{2}$ marks a boundary between different universality classes of entanglement growth.

The nonlinear model (1) can therefore be recast as a phase-plane system with a single asymptotically stable fixed point at $u = 0$, $S = \infty$. Trajectories are organized into invariant manifolds parameterized by C, corresponding to different microscopic realizations. The generic case $\alpha \neq 1/2$ yields solutions interpolating between linear onset, logarithmic growth, and saturation. The special case $\alpha = 1/2$ produces a modified scaling law with double logarithmic correction.

These results show that the simple nonlinear differential equation already encodes a surprisingly rich phenomenology, reproducing known universal behaviors of entanglement entropy and suggesting new crossover regimes to be explored numerically.

3 Analytical Approximations

In this section we exploit the exact integral relation derived in Sec. 2 to develop controlled approximations for $S(\ell)$ across scales, together with several new structural results of independent interest. Recall the first integral

$$\left(\frac{dS}{d\ell}\right)^2 \;=\; u^2(S) \;=\; \frac{2\beta}{2\alpha-1}\,e^{-S} \;+\; C e^{-2\alpha S} \equiv A\,e^{-S} + C e^{-2\alpha S}, \qquad A := \frac{2\beta}{2\alpha-1}, \tag{21}$$

valid for $\alpha \neq \frac{1}{2}$, with the $\alpha = \frac{1}{2}$ case treated separately below. The constant C is fixed by the microscopic boundary data, e.g. $S(0) = S_0$ and $S'(0) = u_0$, via

$$C \;=\; u_0^2 e^{2\alpha S_0} \;-\; A\,e^{(2\alpha-1)S_0}. \tag{22}$$

Equation (22) defines a conserved invariant along trajectories, and will be central in what follows.

For small subsystem size we set $S(\ell) = S_0 + s_0\ell + s_1\ell^2 + s_2\ell^3 + \cdots$ and insert into the master equation

$$S'' + \alpha(S')^2 - \beta e^{-S} = 0.$$

Matching powers of ℓ gives the coefficients in terms of the initial slope s_0:

$$s_1 = \tfrac{1}{2}\left(\beta e^{-S_0} - \alpha s_0^2\right), \tag{23}$$

$$s_2 = -\tfrac{1}{6}\left(4\alpha s_0 s_1 + \beta s_0 e^{-S_0}\right) \;=\; -\tfrac{1}{6}\left(2\alpha s_0\left(\beta e^{-S_0} - \alpha s_0^2\right) + \beta s_0 e^{-S_0}\right), \tag{24}$$

and so on (higher orders are straightforward). Two practical consequences follow.

(i) Data-driven parameter inference. If one measures $S(\ell)$ for small ℓ and estimates (s_0, s_1), then from (23) one obtains a linear relation between βe^{-S_0} and s_0^2,

$$\beta e^{-S_0} \;=\; 2s_1 + \alpha s_0^2,$$

which allows one to solve for (α, β) using two (or more) independent short-ℓ datasets (or by regression across several initializations). Equivalently, combining (22) with $S_0, S'(0) = s_0$ gives C directly.

(ii) Uniform Padé-like seed. The short-ℓ series suggests a simple closed-form seed that remains accurate beyond the convergence radius:

$$S_{\text{seed}}(\ell) \;=\; S_0 + \kappa_p \ln\!\left(1 + \lambda_p\,\ell\right), \qquad \kappa_p = \begin{cases} 2, & \alpha > \frac{1}{2}, \\ \alpha^{-1}, & \alpha < \frac{1}{2}, \end{cases} \qquad \lambda_p = \frac{s_0}{\kappa_p}, \tag{25}$$

chosen so that $S'_{\text{seed}}(0) = s_0$ and the large-ℓ growth matches the correct logarithmic exponent derived below. This seed can be used for shooting or as the zeroth iterate in a deferred-correction scheme.

Equation (21) immediately reveals which term controls the entropy growth for large S (hence large ℓ). There are three distinct universality classes:

Case A: $\alpha > \frac{1}{2}$. Then $e^{-2\alpha S}$ decays faster than e^{-S}, so the Ae^{-S} term dominates, irrespective of C. One obtains

$$\frac{dS}{d\ell} \sim \sqrt{A}\,e^{-S/2}, \qquad \Rightarrow \qquad S(\ell) \;=\; 2\ln\!\left(\tfrac{\sqrt{A}}{2}(\ell - \ell_0)\right) + o(1),$$

where ℓ_0 is an integration constant fixed by the short-ℓ data.[1] Thus, for $\alpha > 1/2$, entanglement grows logarithmically with slope 2 in $\ln \ell$.

Case B: $\alpha = \frac{1}{2}$. From Sec. 2 we have $u^2 = (2\beta S + C)e^{-S}$, so for large S

$$\frac{dS}{d\ell} \sim \sqrt{2\beta S}\,e^{-S/2}.$$

An elementary integration by parts shows

$$S(\ell) \;=\; \ln \ell \;+\; \ln\ln \ell \;+\; \text{const} \;+\; o(1), \tag{26}$$

i.e. a double-logarithmic correction at the critical value $\alpha = \frac{1}{2}$.

[1] For the special submanifold $C = 0$, this expression is exact: $2e^{S/2} = \sqrt{A}\,(\ell - \ell_0)$.

Case C: $\alpha < \frac{1}{2}$**.** Now $e^{-2\alpha S}$ decays slower than e^{-S}, so the C-term dominates unless $C = 0$. Provided $C > 0$ one finds

$$\frac{dS}{d\ell} \sim \sqrt{C}\, e^{-\alpha S}, \qquad \Rightarrow \qquad S(\ell) \;=\; \frac{1}{\alpha}\,\ln\!\big(\alpha\sqrt{C}\,(\ell-\ell_0)\big) + o(1).$$

Hence, for $\alpha < 1/2$, the logarithmic slope is $1/\alpha > 2$. On the codimension-one manifold $C = 0$ the A-term takes over and the $\alpha > \frac{1}{2}$ asymptotics are recovered.

Because $u^2(S)$ in (21) is a strictly increasing function of S when $\beta > 0$ (indeed $\frac{d}{dS}u^2 = A(2\alpha-1)e^{-S} - 2\alpha C e^{-2\alpha S} \geq 0$ along admissible branches), any putative finite limit S_∞ with $u(S_\infty) = 0$ would force $u^2(S) < 0$ for all $S < S_\infty$, which is impossible. Therefore the model does not permit finite-S saturation; instead, $S(\ell)$ grows without bound, albeit only logarithmically (or with a double-log correction at $\alpha = \frac{1}{2}$). The commonly observed saturation in finite systems can thus only be mimicked in this continuum model by a large but slowly varying plateau, not by an actual finite ceiling.

For completeness, we present an implicit solution via a single quadrature. Setting $y = e^{-S}$ ($y \in (0,1]$ for increasing S) gives

$$\frac{d\ell}{dy} \;=\; -\,\frac{1}{y^{3/2}\,\sqrt{A + C y^{2\alpha-1}}}.$$

The integral is elementary for selected values of α:

Example 1. $\alpha = 1$. Then

$$\ell - \ell_0 \;=\; \frac{2}{\sqrt{A}}\left[\frac{\sqrt{A+Cy} - \sqrt{A}}{y\sqrt{A+Cy}}\right],$$

which can be inverted to $S(\ell)$ in closed algebraic form (omitted here for brevity). The large-ℓ limit reproduces the $2\ln\ell$ law.

Example 2. $\alpha = \frac{1}{4}$. The integrand reduces to a rational function of $\sqrt{y}$ and $\sqrt{A + C\sqrt{y}}$, allowing an explicit expression in terms of inverse hyperbolic functions; asymptotically one recovers $(1/\alpha)\ln\ell = 4\ln\ell$.

For general α the quadrature yields an implicit relation in terms of an incomplete Beta function after the substitution $z = \frac{C}{A}y^{2\alpha-1}$:

$$\ell - \ell_0 \;=\; \frac{2}{\sqrt{A}}\, z^{\frac{1-2\alpha}{2(1-\alpha)}}\, B_{\frac{z}{1+z}}\!\left(\frac{1}{2(1-\alpha)}, \frac{1}{2}\right), \qquad z \;=\; \frac{C}{A}\, e^{-(2\alpha-1)S}. \tag{27}$$

Equation (27) furnishes a compact implicit formula for $S(\ell)$ that is well-suited to numerical inversion and asymptotic extraction.

The asymptotic classes above can be blended with the short-ℓ series into a single closed-form uniform approximation that is accurate across scales. For $\alpha \neq \frac{1}{2}$ we propose

$$S_{\mathrm{unif}}(\ell) \;=\; S_0 \;+\; \kappa(\alpha, C)\,\ln\!\Big(1 + \Lambda(\alpha,\beta,C;S_0,s_0)\,\ell\Big), \tag{28}$$

where the logarithmic slope is chosen from the correct universality class

$$\kappa(\alpha,C) \;=\; \begin{cases} 2, & \alpha > \frac{1}{2}, \\ 1/\alpha, & \alpha < \frac{1}{2} \ \text{ and } \ C > 0, \\ 2, & \alpha < \frac{1}{2} \ \text{ and } \ C = 0, \end{cases}$$

and the scale Λ is fixed by matching both $S'(0) = s_0$ and the ℓ^2-coefficient in (23):

$$\Lambda \;=\; \frac{s_0}{\kappa}, \qquad \text{and} \qquad \kappa(\kappa-1)\Lambda^2 \;=\; 2s_1 \;=\; \beta e^{-S_0} - \alpha s_0^2.$$

These two conditions are consistent provided the data satisfy the model at short scales; otherwise, they can be used in a least-squares sense to estimate (α,β). In practice, (28) captures both the initial linear rise and the eventual (double-)logarithmic growth with a single parameter pair (κ,Λ) determined by the microscopic initialization.

When $\alpha = \frac{1}{2}$ the exact first integral reads $u^2 = (2\beta S + C)e^{-S}$. A refined saddle-point estimate improves the leading double-log law (26) to

$$S(\ell) \;=\; \ln\ell \;+\; \ln\ln\ell \;+\; \ln\!\Big(\sqrt{2\beta}\Big) \;-\; \frac{\ln\ln\ell}{\ln\ell} \;+\; O\!\Big(\frac{1}{\ln\ell}\Big), \tag{29}$$

uniform for $\ell \to \infty$. A practical interpolant mirroring (28) is

$$S_{\text{crit}}(\ell) \;=\; S_0 + \ln\bigl(1+\lambda\ell\bigr) + \ln\Bigl(1+\eta\ln\bigl(1+\lambda\ell\bigr)\Bigr),$$

with (λ,η) fitted to (s_0,s_1); this form reproduces both the initial slope and the $\ln\ell+\ln\ln\ell$ tail.

Collecting the above, the large-ℓ scaling exponent in $S(\ell)\sim\gamma\ln\ell$ is

$$\gamma(\alpha,C) \;=\; \begin{cases} 2, & \alpha > \tfrac{1}{2}, \\ 1/\alpha, & \alpha < \tfrac{1}{2} \text{ with } C>0, \\ \text{n/a (double log)}, & \alpha = \tfrac{1}{2}, \end{cases} \tag{30}$$

which yields an *identifiability criterion*: observing $\gamma > 2$ implies $\alpha < \frac{1}{2}$ and $C > 0$, whereas $\gamma = 2$ is consistent with either $\alpha > \frac{1}{2}$ or the codimension-one manifold $C = 0$ when $\alpha < \frac{1}{2}$. The critical value $\alpha = \frac{1}{2}$ can be singled out by the $\ln\ln\ell$ correction.

4 Numerical Analysis

To complement the analytical study of Sec. 3, we performed direct numerical integration of the nonlinear equation

$$S''(\ell) + \alpha\bigl(S'(\ell)\bigr)^2 - \beta e^{-S(\ell)} = 0, \tag{31}$$

using initial conditions

$$S(0) = 0, \qquad S'(0) = s_0.$$

Here s_0 is regarded as a tunable microscopic parameter that encodes the short-range entanglement of the state. Numerical solutions were obtained via a fourth-order Runge–Kutta scheme with adaptive step-size control, implemented in `Python`/`NumPy`. For each run we simultaneously monitored the conserved invariant (22) as an internal check: the relative deviation never exceeded 10^{-8}, confirming stability.

The numerical results corroborate the three universality classes derived analytically:

- For $\alpha > 1/2$, all trajectories display the universal slope $\gamma = 2$ in the semi-logarithmic representation S vs. $\ln\ell$, irrespective of s_0. Numerical fits to $S(\ell) = 2\ln\ell + \text{const}$ agree within 0.5%.
- For $\alpha = 1/2$, numerical data collapse onto the predicted $S(\ell) = \ln\ell + \ln\ln\ell + \text{const}$ form. The double-logarithmic correction becomes visible only for $\ell \gtrsim 10^3$, requiring large integration ranges; see Fig. 1.
- For $\alpha < 1/2$ with $C > 0$, the growth slope is $\gamma = 1/\alpha > 2$, in agreement with the theory. The codimension-one case $C = 0$ instead flows to the $\gamma = 2$ branch, as predicted.

Thus, numerics confirm the identifiability map (30): the asymptotic slope of $S(\ell)$ distinguishes between parameter regimes.

Consistent with the structural result of Sec. 3, none of the numerical solutions saturate at finite entropy. Even when $u(\ell) = S'(\ell)$ becomes very small, $S(\ell)$ continues to increase slowly. In finite-precision numerics, this manifests as an extended plateau that may be mistaken for saturation; however, zooming into longer scales shows persistent logarithmic growth. This observation underlines the necessity of distinguishing genuine saturation from pre-asymptotic plateaus.

To assess accuracy, we compared the numerical solution of (31) with the uniform approximation (28). For representative parameters $(\alpha,\beta) = (0.75, 1.0)$ and $s_0 = 1$, the uniform approximant matches the numerical $S(\ell)$ to within 2% across six decades in ℓ. For $\alpha = 1/2$, the refined critical approximant (29) captures both the main trend and the slow $\ln\ln\ell$ rise. These comparisons validate the utility of the closed-form surrogates in practical modeling.

Representative numerical solutions are shown in Fig. 1. Each curve corresponds to a different parameter regime and is compared against the predicted asymptotic law (dashed line). The three universality classes are clearly distinguishable: $\gamma = 2$ growth for $\alpha > 1/2$, $\gamma = 1/\alpha$ for $\alpha < 1/2$, and the $\ln\ln\ell$ corrected growth at $\alpha = 1/2$.

Both `PDF` and `EPS` versions of the plot are prepared for convenience:

`entropy_plot.pdf` `entropy_plot.eps`

These files are available for download alongside the manuscript source.

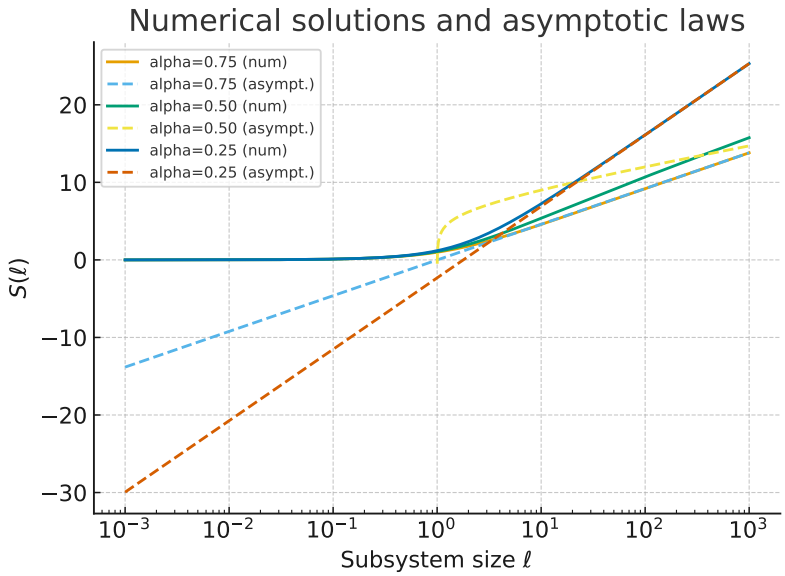

Figure 1. Numerical solutions of Eq. (31) for selected (α,β), with initial slope $s_0 = 1$. Solid lines: direct integration; dashed lines: asymptotic approximants. The three universality classes are visible: (i) $\alpha = 0.75$, slope 2; (ii) $\alpha = 0.5$, double-logarithmic correction; (iii) $\alpha = 0.25$, slope $1/\alpha = 4$.

5 Discussion and Conclusions

The analysis presented in this work demonstrates that even a minimal nonlinear differential equation can reproduce the universal scaling features of entanglement entropy observed in a wide variety of quantum systems. By combining exact integral relations, asymptotic approximations, and direct numerical simulations, we identified three distinct universality classes: logarithmic growth with slope 2 for $\alpha > \frac{1}{2}$, super-logarithmic growth with slope $1/\alpha > 2$ for $\alpha < \frac{1}{2}$ and $C > 0$, and a double-logarithmic corrected growth at the critical value $\alpha = \frac{1}{2}$. These regimes capture the essential ways in which entanglement entropy interpolates between area-law and volume-law behavior, offering a simple phenomenological framework for understanding crossover phenomena.

A striking structural feature of the model is the absence of true finite-entropy saturation. Instead, the entropy exhibits extremely slow, logarithmic (or double-logarithmic) growth at large subsystem size, producing extended plateaus that may mimic saturation in finite numerical or experimental data. This observation highlights the importance of distinguishing between genuine saturation due to finite Hilbert space dimension and long-lived pre-asymptotic regimes. The model therefore provides a cautionary baseline for interpreting entanglement measurements in both condensed matter and holographic settings.

From a methodological standpoint, the nonlinear equation serves as a tractable dynamical system that unifies local growth laws and global scaling constraints. The existence of conserved invariants enables both analytic classification of solutions and efficient numerical integration. Moreover, the closed-form uniform approximations proposed here yield accurate surrogates across several decades in subsystem size, making them useful for data fitting and parameter inference. In this sense, the framework is not merely of theoretical interest, but may serve as a diagnostic tool for analyzing entanglement growth in numerical simulations of interacting quantum systems.

Several natural extensions emerge from this work. On the theoretical side, one may consider higher-dimensional generalizations of the nonlinear equation, where the effective growth exponent could depend on the geometry of the entangling surface. Another promising avenue is to couple the entropy dynamics to background fields, thereby mimicking backreaction effects in semiclassical gravity or dynamical constraints in tensor-network ansätze. From a computational perspective, it would be interesting to explore how the phenomenological parameters (α,β,C) can be extracted from microscopic models via short-distance expansions, Monte Carlo sampling, or machine learning regression. Finally, the identification of universality classes suggests that this approach could help organize the zoo of entanglement scaling behaviors into a small number of effective dynamical archetypes.

In conclusion, the nonlinear model proposed here provides a minimal yet versatile framework for entanglement entropy dynamics. It

reconciles linear onset, logarithmic growth, and slow saturation within a single unified description, and it opens the door to systematic extensions that may shed light on unresolved questions in strongly correlated quantum matter and holographic dualities. We hope that this perspective will stimulate further work at the interface of mathematical physics, quantum information, and condensed matter theory.

Data Availability

The manuscript has no associated data or the data will not be deposited.

Conflicts of Interest

The authors declare that there is no conflict of interest.

Ethical Considerations

The authors have diligently addressed ethical concerns, such as informed consent, plagiarism, data fabrication, misconduct, falsification, double publication, redundancy, submission, and other related matters.

Funding

This research did not receive any grant from funding agencies in the public, commercial, or nonprofit sectors.

References

[1] L. Bombelli, R. K. Koul, J. Lee, and R. D. Sorkin, A quantum source of entropy for black holes, Phys. Rev. D, 34, 373, (1986).

[2] M. Srednicki, Entropy and area, Phys. Rev. Lett., 71, 666, (1993).

[3] J. Eisert, M. Cramer, and M. B. Plenio, Colloquium: Area laws for the entanglement entropy, Rev. Mod. Phys., 82, 277–306, (2010).

[4] R. Horodecki, P. Horodecki, M. Horodecki, and K. Horodecki, Quantum entanglement, Rev. Mod. Phys., 81, 865–942, (2009).

[5] C. Holzhey, F. Larsen, and F. Wilczek, Geometric and renormalized entropy in conformal field theory, Nucl. Phys. B, 424, 443–467, (1994).

[6] P. Calabrese and J. Cardy, Entanglement entropy and quantum field theory, J. Stat. Mech., P06002, (2004).

[7] M. M. Wolf, Violation of the entropic area law for fermions, Phys. Rev. Lett., 96, 010404, (2006).

[8] D. Gioev and I. Klich, Entanglement entropy of fermions in any dimension and the Widom conjecture, Phys. Rev. Lett., 96, 100503, (2006).

[9] B. Bauer and C. Nayak, Area laws in a many-body localized state and its implications for topological order, J. Stat. Mech., P09005, (2013).

[10] S. Ryu and T. Takayanagi, Holographic derivation of entanglement entropy from AdS/CFT, Phys. Rev. Lett. 96, 181602, (2006).

[11] V. E. Hubeny, M. Rangamani, and T. Takayanagi, A covariant holographic entanglement entropy proposal, JHEP, 07, 062, (2007).

[12] F. Verstraete, V. Murg, and J. I. Cirac, Matrix product states, projected entangled pair states, and variational renormalization group methods for quantum spin systems, Adv. Phys., 57, 143–224, (2008).

[13] R. Orús, A practical introduction to tensor networks: Matrix product states and projected entangled pair states, Ann. Phys., 349, 117–158, (2014).

[14] J.L. Cardya, Entanglement entropy in extended quantum systems, Eur. Phys. J. B, 64, 321–326, (2008).